Computational Aerodynamics for Aircraft Design *

Antony Jameson †

Abstract

This article outlines some of the principal issues in the development of numerical methods for the prediction of flows over aircraft and their use in the design process. These include the choice of an appropriate mathematical model, the design of shock-capturing algorithms, the treatment of complex geometric configurations, and shape modifications to optimize the aerodynamic performance.

While computational methods for simulating fluid flow have by now penetrated a broad variety of fields, including ship design, car design, studies of oil recovery, oceanography, meteorology, and astrophysics, they have assumed a dominant role in aeronautical science. In the aircraft industry there is often a very narrow margin between success and failure. In the past two decades the development of new commercial aircraft successful enough to make a profit for the manufacturer has proved an elusive goal. The economics of aircraft operation are such that even a small improvement in efficiency can translate into substantial savings in operational costs. Therefore, the operating efficiency of an airplane is a major consideration for potential buyers. This provides manufacturers with a compelling incentive to design more efficient aircraft.

One route toward this goal is more precise aerodynamic design with the aid of computational simulation. In particular it is possible to attempt predictions in the transonic flow regime that is dominated by nonlinear effects, exemplified by the formation of shock waves. The importance of the transonic regime stems from the fact that to a first approximation, cruising efficiency is proportional to ML/D, where M is the Mach number (speed divided by the speed of sound), L is the lift, and D is the drag. As long as the speed is well below the speed of sound, the lift-to-drag ratio does not vary much with speed, so it pays to increase the speed until the effects of compressibility start to cause a radical change in the flow. This occurs when embedded pockets of supersonic flow appear, generally terminating in shock waves. A typical transonic flow pattern over a wing is illustrated in Fig. 1. As the Mach number is increased the shock waves become strong enough to cause a sharp increase in drag, and finally the pressure rise through the shock waves becomes so large that the boundary layer separates. The most efficient cruising speed is usually in the transonic regime just at the onset of drag rise, and the prediction of aerodynamic properties in steady transonic flow has therefore been a key challenge.

Prior to 1965 computational methods were hardly used in aerodynamic analysis, although they were widely used for structural analysis. There was already in place a rather comprehensive mathematical formulation of fluid mechanics. This had been developed by elegant mathematical analysis, frequently guided by brilliant insights. Well-known examples include the airfoil theory of Kutta and Joukowski, Prandtl's wing and boundary layer theories, von Karman's analysis of the vortex street, and more recently Jones's slender wing theory (1), and Hayes's theory of linearized supersonic flow (2). These methods, however, required simplifying assumptions of various kinds, and could not be used to make quantitative predictions of complex flows dominated by nonlinear effects. The primary tool for the development of aerodynamic configurations was the wind tunnel. Shapes were tested and modifications selected in the light of pressure and force measurements together with flow visualization techniques. In much the same way that Brunelleschi could design the dome of the Florence cathedral through

*Reprinted from Science, Volume 245, pp. 361-371, 1989

†The author is McDonnell, Professor of Aerospace Engineering, Princeton, NJ 08544

a good physical understanding of load paths, so could experienced aerodynamicists arrive at efficient shapes through testing guided by good physical insight. Notable examples of the power of this method include the achievement of the Wright brothers in leaving the ground (after first building a wind tunnel), and more recently Whitcomb's discovery of the area rule for transonic flow (3). In fact, in the 80 years since the Wright brothers' flight, every conceivable configuration has been tried, and by a process of natural selection airplanes have very rapidly evolved to the rather efficient forms we see flying today.

Experimental design is an expensive process, however. More than 20,000 hours of wind tunnel testing were expended in the development of some modern designs such as the General Dynamics F 111 or the Boeing 747. The computer opens up new possibilities for attacking these problems by direct calculation of solutions to more complete mathematical models. The requirements to be met by an effective method include: (i) capability to simulate the main features of the flow, such as shock waves and vortex sheets; (ii) prediction of viscous effects; (iii) ability to handle geometrically complex configurations; and (iv) efficiency in both computational and human effort.

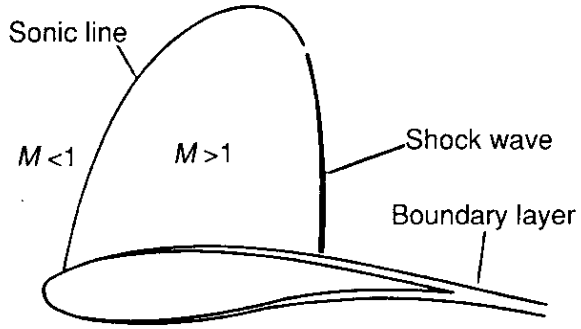

Figure 1: Pattern of transonic flow past an airfoil. The sonic line is where $M = 1$, that is, where the speed equals the speed of sound

This is a formidable list that poses a severe challenge to the numerical analyst. Aside from the need to treat nonlinear effects, the problem is also compounded by the fact that the steady flow equations are of mixed type, elliptic in the subsonic regions of the flow, and hyperbolic in the supersonic regions. Moreover, they are to be solved in the unbounded domain exterior to the aircraft. The problem is somewhat alleviated, however, by the fact that airplanes fly by achieving controlled and steady flows. In some ways it is easier to predict the flow past an airplane than the flow past a nonspinning baseball. The trajectory of a knuckle ball is unpredictable because vortices may be shed at any angle to the axis of flight. Experimental measurements of the drag coefficient of a sphere show drastic variations with speed associated with changes in the wake pattern (4). There is a sudden reduction in the drag coefficient from around 0.4 to around 0.09 when the flow becomes turbulent and the flow separates further aft. Accurate prediction of the drag coefficient would thus require prediction of the change in the separation point as the flow becomes turbulent. The flow past an aircraft is generally attached in normal operating conditions, with the exception of certain high-speed aircraft which use controlled separation off sharp side edges to generate vortices which pass above the wing, thus enhancing the lift. Otherwise the onset of separation typically marks the limits of the flight envelope, such as the stalling point. Consequently, depending on the intended application, useful aerodynamic simulations can be achieved with substantially simplified mathematical models.

This article outlines some of the key issues in the development of algorithms for fluid flow simulation, and their use for aircraft design. The volume of work in computational fluid dynamics precludes a comprehensive review in an article of this length, and the choice of topics must necessarily be personal. Some representative examples of flow calculations have been drawn from the work of the author and his associates.

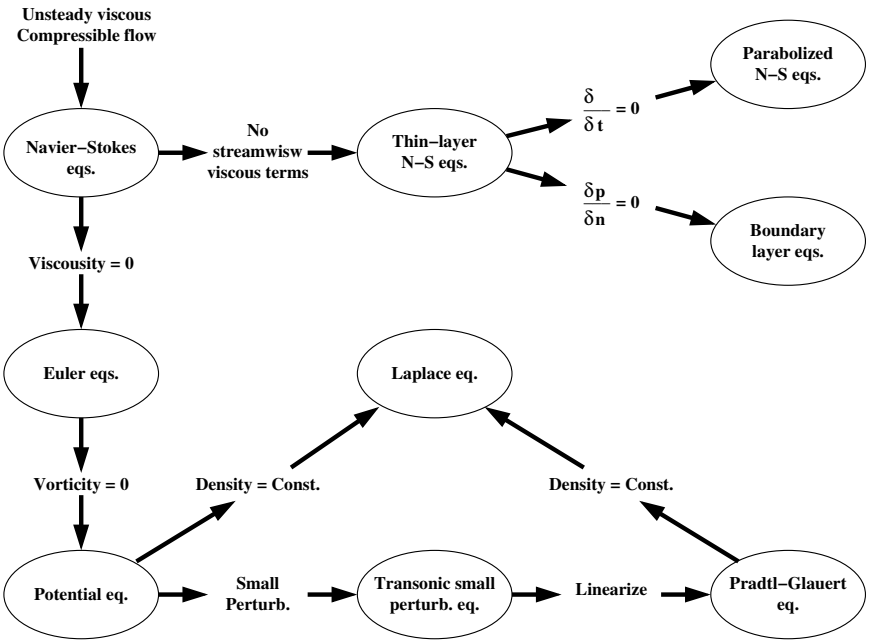

Figure 2: Equations of fluid dynamics for mathematical models of varying complexity. (Supplied by Luis Miranda, Lockheed Corporation)

Mathematical Models of Fluid Flow

The Navier-Stokes equations state the laws of conservation of mass, momentum, and energy for the flow of a gas in thermodynamic equilibrium. In the Cartesian tensor notation, let x_i, be the coordinates, p, ρ, T, and E the pressure, density, temperature, and total energy, and u, the velocity components. Each conservation equation has the form

$$\frac{\partial w}{\partial t} + \frac{\partial F_j}{\partial x_j} \tag{1}$$

For the mass equation

$$w = \rho, \quad F_j = \rho u_j \tag{2}$$

For the i momentum equation

$$w_i = \rho u_i, \quad F_{ij} = \rho u_i u_j + p\delta_{ij} - \sigma_{ij} \tag{3}$$

where σ_{ij} is the visous stress tensor, which is proportional to the rate of strain tensor and the bulk dilatation. If μ and λ are the coefficients of viscosity and bulk viscosity then

$$\sigma_{ij} = \mu\left(\frac{\partial u_i}{\partial x_j} + \frac{\partial u_j}{\partial x_i}\right) + \lambda\delta_{ij}\left(\frac{\partial u_k}{\partial x_k}\right) \tag{4}$$

Usually $\lambda = -2\mu/3$. For the energy equation

$$w = \rho E, \quad F_j = (\rho E + p)u_j - \sigma_{jk}u_k - \kappa\frac{\partial T}{\partial x_j} \tag{5}$$

where κ is the coefficient of heat conduction. The pressure is related to the density and energy by equation of state

$$p = (\gamma - 1)\rho\left(E - \frac{1}{2}u_i u_i\right) \tag{6}$$

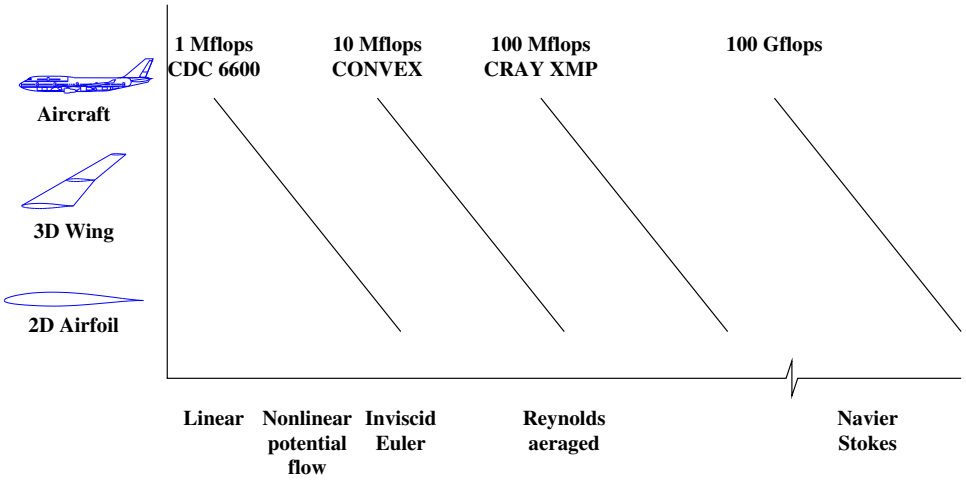

Figure 3: Complexity of the problems that can be treated with different calsses of computer (1 flop=1 floating-point operation per second; 1Mflop = 10^6 flops, 1 Gflop=10^9 flops)

in which γ is the ratio of specific heats.

An indication of the relative magnitude of the internal and viscous terms is given by the Reynold's number

$$R_e = \frac{\rho U L}{\mu} \tag{7}$$

where U is a characteristic velocity and L a representative length. The viscosity of air is very small, and typical Reynolds numbers for the flow past a component of an aircraft such as a wing are of the order of 10^7 or more, depending on the size and speed of the aircraft. In this situation the viscous effects are essentially confined to thin boundary layers covering the surface. Boundary layers may nevertheless have a global impact on the flow by causing separation. Unfortunately, unless they are controlled by active means such as suction through a porous surface, boundary layers are unstable and generally become turbulent.

The computational requirements for the full simulation of all scales of turbulence have been estimated as growing proportionally to $R_e^{9/4}$ (5), and are clearly beyond the reach of current computers. Turbulent flows may be simulated by the Reynolds equations, in which statistical averages are taken of rapidly fluctuating components. Denoting fluctuating parts by primes and averaging by an overbar, this leads to the appearance of Reynolds stress terms of the form $\overline{\rho u_i' u_j'}$ which cannot be determined from the mean values of the velocity and density. Estimates of these additional terms must be provided by a turbulence model. The simplest turbulence models augment the molecular viscosity by an eddy viscosity that crudely represents the effects of turbulent mixing, and is estimated with some characteristic length scale such as the boundary layer thickness. A rather more elaborate class of models introduces two additional equations for the turbulent kinetic energy and the rate of dissipation. Existing turbulence models are adequate for particular classes of flow for which empirical correlations are available, but they are generally not capable of reliably predicting more complex phenomena, such as shock wave-boundary layer interaction. Outside the boundary layer excellent predictions can be made by treating the flow as inviscid. Setting $\sigma_{ij} = 0$ and eliminating heat conduction from Eqs. 2, 3, and 5 yields the inviscid Euler equations, which are a very useful model for predicting flows over aircraft. According to Kelvin's theorem, a smooth inviscid flow that is initially irrotational remains irrotational. This allows one to introduce a velocity potential 4 such that $u_i = \partial\Phi/\partial x_i$. The Euler equations for a steady flow now reduce to

$$\frac{\partial}{\partial x_i}\left(\rho \frac{\partial \Phi}{\partial x_i}\right) = 0 \tag{8}$$

This may be expanded in quasilinear form as

$$c^2 \frac{\partial^2 \Phi}{\partial x_i^2} - u_i u_j \frac{\partial^2 \Phi}{\partial x_i \partial x_j} = 0 \tag{9}$$

where c is the speed of sound, which is determined by the relation $c^2 = \gamma p/\rho$

If the flow is locally aligned, say, with the x_1 axis, Eq. 9 reads as

$$(1 - M^2)\frac{\partial^2 \Phi}{\partial x_i^2} + \frac{\partial^2 \Phi}{\partial x_2^2} + \frac{\partial^2 \Phi}{\partial x_3^2} \tag{10}$$

where M is the Mach number u_1/c. The change from an elliptic to a hyperbolic partial differential equation as the flow becomes supersonic is evident. According to Crocco's theorem (6), the vorticity g in a steady flow is related to entropy production through the relation $\mathbf{u}$ x $\xi + T\nabla S = 0$, where S is the entropy. Thus the introduction of a potential is consistent with the assumption of isentropic flow. If M_∞ is the free stream Mach number, then $p = \rho^\gamma/\gamma M_\infty^2$ and $\rho = (M_\infty c^2)^{1/(\gamma-1)}$

The potential flow equation cannot exactly model shock waves, through which entropy is produced. Weak solution admitting isentropic jumps that conserve mass but not momentum are a good approximation to shock waves, however, as long as the shock waves are quite weak (with a Mach number ¡ 1.3 for the normal velocity component upstream of the shock wave). Stronger shock waves tend to separate the flow, with the result that the inviscid approximation is no longer adequate. Thus this model well balanced, and it has proved extremely useful for the prediction of the cruising performance of transport aircraft. An estimate of the pressure drag arising from shock waves is obtained because of the momentum deficit through an isentropic jump.

If one assumes small disturbances about a free stream in the x_1 direction, and a Mach number close to unity, Eq. 10 can be reduced to the transonic small disturbance equation in which M^2 is estimated as

$$M_\infty^2[1 - (\gamma + 1)\partial\Phi/\partial x_1]$$

The final level of approximation is to linearize Eq. 10 by replacing M^2 by its free stream value M_∞. In the subsonic case the resulting Prandtl-Glauert equation can be reduced to Laplace's equation by scaling the x, coordinate by $(1 - M_\infty^2)^{1/2}$. Ideal incompressible flow satisfies the Laplace's equation, as can be seen by setting $\rho =$ constant in Eq. 8.

The hierarchy of mathematical models is illustrated in Fig. 2. With limits on the available computing power, and the cost of the calculations, one has to make a trade-off between the complexity of the mathematical model and the complexity of the geometric configuration to be treated. The first major success in computational aerodynamics was the development of boundary integral methods (7, 8), which enabled the linearized potential flow equation to be solved routinely for arbitrary configurations. In the 1970s effective methods were devised for the treatment of the transonic potential flow equation (9-13). These were instrumental, for example, in the development of refined wing designs for aircraft such as the Canadair Challenger and the Boeing 757, and they are still widely used today. More recently there have been intensive efforts to develop good algorithms for the Euler and Navier-Stokes equations.

The computational requirements for aerodynamic simulation are a function of the number of operations required per mesh point, the number of cycles or time steps needed to reach a solution, and the number of mesh points needed to resolve the important features of the flow. Algorithms for the three-dimensional transonic potential flow equation require about 500 floating point operations per mesh point per cycle. The number of operations required for an Euler simulation is in the range of 1000 to 5000 per time step, depending on the complexity of the algorithm. The number of mesh intervals required to provide an accurate representation of a two-dimensional inviscid transonic flow is of the order of 160 wrapping around the profile, and 32 normal to the airfoil. Correspondingly, about 100,000 mesh cells are sufficient to provide adequate resolution of three-dimensional inviscid transonic flow past a swept wing, and this number needs to be increased to provide a good simulation of a more complex configuration such as a complete aircraft. The requirements for viscous simulations by means of turbulence models are much more severe. Good resolution of a turbulent boundary layer needs

about 32 intervals inside the boundary layer, with the result that a typical mesh for a two-dimensional Navier-Stokes calculation contains 512 intervals wrapping around the profile, and 64 intervals in the normal direction. A corresponding mesh for a swept wing would have, say, 512 X 64 X 256 = 8,388,608 cells, leading to a calculation at the outer limits of current computing capabilities. Figure 3 gives an indication of the boundaries of the complexity of problems with can be treated with different levels of computing power. The vertical axis indicates the geometric complexity, and the horizontal axis the equation complexity.

Algorithms for Flow Simulation

The case of the inviscid Euler equations is used here to illustrate a general approach to the design of algorithms for aerodynamic simulation (14). The underlying idea is simply to integrate the timedependent equations of fluid flow until the solution evolves to a steady state. This may be accomplished by dividing the domain of the flow into a large number of small subdomains and applying the conservations laws in integral form

$$\frac{\partial}{\partial t}\int_{\Omega} w d\Omega + \int_{\partial\Omega} \mathbf{F}.\mathbf{dS} = 0 \tag{11}$$

Here $\mathbf{F}$ is the vector appearing in Eq. 1, and $\mathbf{dS}$ is the directed surface element of the boundary $d\Omega$ of the domain Ω. The use of the integral form has the advantage that no assumption of the differentiability of the solutions is implied, with the result that it remains a valid statement for a domain containing a shock wave. In general the subdomains could be arbitrary, but it is convenient to use either hexahedral or tetrahedral cells. Hexahedral cells are naturally generated by the use of body conforming meshes corresponding to curvilinear coordinate systems. Where the geometric complexity of the configuration is such that it becomes difficult to generate a structured mesh of this kind, one may prefer to resort to an unstructured decomposition into tetrahedral cells. Alternative discretization schemes may be derived by storing sample values of the flow variables at either the cell centers or the cell vertices.

With a tetrahedral mesh, each face is a common external boundary to exactly two control volumes. Therefore each internal face can be associated with a set of five mesh points consisting of its three corners 1, 2, and 3, and the vertices 4 and 5 of the two tetrahedra based on the face. Vertices 4 and 5 are the centers of the two control volumes influenced by the face. It is now possible to generate the discrete approximation by presetting the flux balance at each mesh point to zero, and then performing a single loop over the faces. For each face one first calculates the fluxes of mass, momentum and energy across the face, and then one assigns these contributions to the vertices 4 and 5 with positive and negative signs, respectively. Because every contribution is transferred from one control volume into another, all quantities are perfectly conserved. Mesh points on the inner and outer boundaries lie on the surface of their own control volumes, and the accumulation of the flux balance in these volumes has to be correspondingly modified.

An alternative route to the discrete equations if provided by the Galerkin Method. Multiplying Eq. 1 by a test function ϕ, and integrating by parts over space, one obtains the weak form

$$\frac{\partial}{\partial t}\int\int\int_{\Omega} \phi w d\Omega = \int\int\int_{\Omega} \mathbf{F}.\nabla\phi d\Omega - \int\int_{\partial\Omega} \phi \mathbf{F}.\mathbf{dS} \tag{12}$$

that is also valid in the presence of discontinuities in the flow. By choosing test functions with local support, separate equations are obtained for each node. For example, if ϕ is piecewise linear, with a nonzero value only at a single node, and one also assumes that flux vector to be piecewise linear, one obtains a flux balance for the node that is equivalent to the use of trapezoidal integration in the integral conservation law.

These procedures lead to nondissipative approximations to the Euler equations. Dissipative terms may be needed for two reasons. First there is the possibility of frozen oscillatory modes. The second reason is to allow the clean capture of shock waves and contact discontinuities without undesirable oscillations. An extreme overshoot could resultogn a negative value of an inherently positive quantity such as the pressure or density.

Consider a general semidiscrete scheme of the form

$$\frac{d}{dt}v_j = \sum_k c_{jk}(v_k - v_j) \tag{13}$$

A maximum cannot increase and a minimum cannot decrease if the coefficients c_{jk} are nonnegative. Positivity conditions of this type lead to diagonally dominant schemes, and they are a key to the elimination of unwanted oscillations. They may be realized by the introduction of dissipative terms or by the use of upwind biasing in the discrete scheme. Unfortunately they may also lead to severe restrictions on the accuracy unless the coefficients have a complex nonlinear dependence on the solution.

Following the pioneering work of Godunov (15), a variety of dissipative and upwind schemes designed to have good shock capturing properties have been developed during the past decade (16-25). The one-dimensional scalar conservation law

$$\frac{du}{dt} + \frac{\partial}{\partial x}f(u) = 0 \tag{14}$$

provides a useful method for the analysis of these schemes. The total variation

$$\int_{-\infty}^{\infty} \left|\frac{\partial u}{\partial x}\right| dx$$

of a solution of this equation does not increase, provided that any discontinuity appearing in the solution satisfies an entropy condition (24). Harten proposed that difference schemes ought to be designed so that the total variation cannot increase (19). General conditions on coefficients which result in total variation diminishing (TVD) for schemes of this kind were stated and proved by Jameson and Lax (27), and also by Osher and Chakravarthy (28). In the case of a three-point scheme they are equivalent to the positivity conditions stated above.

A conservative semidiscrete approximation to the one dimensional conservation law can be derived by subdividing the line into cells. Then the evolution of the value vj in the jth cell is given by

$$\Delta x \frac{d}{dt}v_j + h_{j+1/2} - h_{j-1/2} = 0 \tag{15}$$

where $h_{j+1/2}$ is an estimate of the flux between cells j and j+1. The simplest estimate is the average $(f_{j+1}+f_j)/2$ but this leads to a scheme that does not satisfy the positivity conditions. To correct this one may add a dissipative term and set

$$h_{j+1/2} = \frac{1}{2}(f_{j+1} + f_j) + \alpha_{j+1/2}(v_j - v_{j-1}) \tag{16}$$

In order to estimate the required value of the coefficient $\alpha_{j+1/2}$, let $a_{j+1/2}$ be a numerical estimate of the wave speed $\partial f/\partial u$,

$$a_{j+1/2} = \begin{cases} \frac{f_{j+1}-f_j}{v_{j+1}-v_j} \text{ if } v_{j+1} \neq v_j \\ \frac{\partial f}{\partial v}\Big| v = v_j \text{ if } v_{j+1} = v_j \end{cases} \tag{17}$$

Now

$$\begin{aligned} h_{j+1/2} &= f_j + (f_{j+1} - f_j)/2 - \alpha_{j+1/2}(v_{j+1} - v_j) \\ &= f_j - (\alpha_{j+1/2} - \frac{1}{2}a_{j+1/2})(v_{j+1} - v_j) \end{aligned} \tag{18}$$

and similarly

$$h_{j-1/2} = f_j - (\alpha_{j-1/2} + \frac{1}{2}a_{j-1/2})(v_j - v_{j-1}) \tag{19}$$

Thus the positivity conditions are satisfied if

$$\alpha_{j+1/2} \geq \frac{1}{2}\left|a_{j+1/2}\right|$$

for all j. The minumum sufficient value of just one half the wave speed produces the upwind scheme

$$h_{j+1/2} = \begin{cases} f_j & \text{if } a_{j+1/2} \geq 0 \\ f_{j+1} & \text{if } a_{j+1/2} < 0 \end{cases} \tag{20}$$

It may be noted that the successful treatment of transonic potential flow also involved the use of upwind biasing. This was first introduced by Murman and Cole to treat the transonic small disturbance equation (9). The author's rotated difference scheme (10), which extended their technique to treat the general transonic potential flow equation, proved to be very robust. TVD schemes can yield sharp discrete shock waves without oscillations, but in this simple form they are at best first-order accurate. Schemes that are second-order accurate almost everywhere can be devised with the aid of flux limiters. These are used to limit the magnitude of higher order antidiffusive or corrective terms depending on the ratio of the differences $\Delta_{j+1/2} = v_{j+1} - v_j$, and $\Delta_{j-1/2}$ in adjacent cells. This technique may be traced to the work of Boris and Book (16), and it was also independently advanced by van Leer (17).

In order to apply these ideas to a system of equations one may split the flux into components corresponding to the different wave speeds. A convenient way to do this was proposed by Roe (19). Another promising approach is to reduce the multidimensional Euler equations directly to a diagonal form (29, 30). The use of flux splitting allows the precise matching of the dissipative terms to introduce the minimum amount of dissipation needed to prevent oscillations, but it is computationally expensive. In practice the use of a blend of low- and high-order dissipative terms with adaptive coefficients conditioned to the maximum local wave speed can yield effective shock capturing schemes. Recently Engquist, Lotstedt, and Sjogreen have shown that oscillations can be effectively controlled by post-processing the result after each time step with a filter which is applied only if a new extremum is detected (31). These procedures lead to a set of coupled ordinary differential equations, which can be written in the form

$$\frac{d\mathbf{w}}{dt} + \mathbf{R}(\mathbf{w}) = 0 \tag{21}$$

where $\mathbf{w}$ is the vector of the flow variables at the mesh points, and $\mathbf{R(w)}$ is the vector of the residuals, consisting of the flux balances defined by the space discretization scheme, together with the added dissipative terms. These are to be integrated to a steady state. If the objective is simply to reach the steady state and details of the transient solution are immaterial, the time-stepping scheme may be designed solely to maximize the rate of convergence. The first decision is whether to use an explicit scheme, in which the space derivatives are calculated from known values of the flow variables at the beginning of the time step, or an implicit scheme, in which the formulas for the space derivatives include as yet unknown values of the flow variables at the end of the time step, leading to the need to solve coupled equations for the new values. The permissable time step of an explicit scheme is limited by the Courant-Friedrichs-Lewy (CFL) condition, which states that a difference scheme cannot be a convergent and stable approximation unless its domain of dependence contains the domain of dependence of the corresponding differential equation (32).

One can anticipate that implicit schemes will yield convergence in a smaller number of time steps, because the time step is no longer constrained by the CFL condition. This will be efficient, however, only if the decrease in the number of time steps outweighs the increase in the computational effort per time step consequent upon the need to solve coupled equations. The prototype implicit scheme can be formulated by estimating $\partial \mathbf{w}/\partial t$ at $t + \mu\Delta t$ as a linear combination of $\mathbf{R}(\mathbf{w}^n)$ and $\mathbf{R}(\mathbf{w}^{n+1})$. The resulting equation

$$\mathbf{w}^{n+1} = \mathbf{w}^n - \Delta t \left\{ (1-\mu)\mathbf{R}(\mathbf{w}^n) + \mu \mathbf{R}(\mathbf{w}^{n+1}) \right\} \tag{22}$$

can be linearized as

$$\left(\mathbf{I} + \mu \Delta t \frac{\partial \mathbf{R}}{\partial \mathbf{w}} \right) \delta \mathbf{w} + \Delta t \mathbf{R}(\mathbf{w}^n) = 0 \tag{23}$$

This reduces to the Newton iteration if one sets $\mu = 1$ and lets $\Delta t \to \infty$. In a three dimensional case with an N x N x N mesh its bandwidth is of order N^2. Direct inversion requires a number of operations proportional to the number of unknowns multiplied by the square of the bandwidth, that is, of the order of N^7. This is prohibitive, and forces recourse to either an approximate factorization method or an iterative solution method.

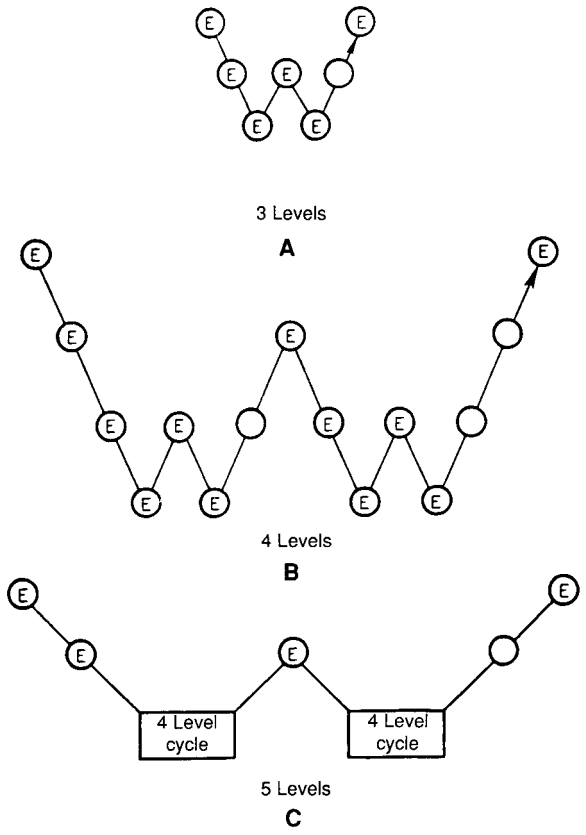

Figure 4: Multigrid W cycle for managing the grid calculation. Symbols: E, calculate the change in flow for one time step, ∘, transfer the data without updating the solution

Alternating direction methods, which introduce factors corresponding to each coordinate, are widely used for structured rectangular meshes (33, 34), but they cannot be implemented on unstructured tetrahedral meshes that do not contain identifiable mesh directions. If one chooses to adopt the iterative solution technique, the principal alternatives are variants of the Gauss-Seidel and Jacobi methods. A symmetric Gauss-Seidel method with one iteration per time step is essentially equivalent to an approximate lower-upper (LU) factorization of the implicit scheme (35-37). On the other hand the Jacobi method with a fixed number of iterations per time step reduces to a multistage explicit scheme, belonging to the general class of Runge-Kutta schemes (38). Schemes of this type have proved very effective for wide variety of problems, and they have the advantage that there can be applied equally easily on both structured and unstructured meshes (39-42).

Let $\mathbf{w}^n$ be the result after n steps. The general form of an m stage scheme is

$$\begin{array}{rcl} \mathbf{w}^{(0)} & = & \mathbf{w}^n \\ \mathbf{w}^{(1)} & = & \mathbf{w}^{(0)} - \alpha_1 \Delta t \mathbf{R}^{(0)} \\ \cdots & & \\ \mathbf{w}^{(m-1)} & = & \mathbf{w}^{(0)} - \alpha_{m-1} \Delta t \mathbf{R}^{(m-2)} \\ \mathbf{w}^{(m)} & = & \mathbf{w}^{(0)} - \Delta t \mathbf{R}^{(m-1)} \\ \mathbf{w}^{(n+1)} & = & \mathbf{w}^{(m)} \end{array} \tag{24}$$

In cases where only the steady state solution is needed, it is helpful to separate the residual $\mathbf{R(w)}$ into its convective and dissipative parts $\mathbf{Q(w)}$ and $\mathbf{D(w)}$. Then the residual in the (q+1)st stage is evaluated as

$$\mathbf{R}^{(q)} = \sum_{r=0}^{4} \left\{ \beta_{qr} \mathbf{Q}(\mathbf{w}^{(r)}) - \gamma_{qr} \mathbf{D}(\mathbf{w}^{(r)}) \right\} \tag{25}$$

where

$$\sum_{r=0}^{4} \beta_{qr} = 1, \quad \sum_{r=0}^{4} \gamma_{qr} = 1$$

Blended multistage schemes of this type, which have been analyzed elsewhere (42), can be tailored to give large stability intervals along both the imaginary and negative real axes.

Radical further improvements in the rate of convergence to a steady state can be realized by the multigrid time-stepping technique. The concept of acceleration by the introduction of multiple grids was first proposed by Federenko (43). There is by now a fairly well-developed theory of multigrid methods for elliptic equations (44, 45), based on the concept of the updating scheme acting as a smoothing operator on each grid. This theory does not hold for hyperbolic systems. Nevertheless, it seems that it ought to be possible to accelerate the evolution of a hyperbolic system to a steady state by using large time steps on coarse grids so that disturbances will be more rapidly expelled through the outer boundary. Several multigrid time-stepping schemes designed to take advantage of this effect have been proposed (46-50).

One can devise a multigrid scheme using a sequence of independently generated coarser meshes that are not associated with each other in any way. In the case of a structured mesh it is convenient, however, to generate the coarser meshes by eliminating alternate points in each coordinate direction. In order to give a precise description of the multigrid scheme subscripts may be used to indicate the grid. Several transfer operations need to be defined. First the solution vector on grid k must be initialized as

$$w_k^{(0)} = T_{k,k-1} w_{k-1} \tag{26}$$

where w_{k-1} is the current value on grid $k-1$, and $T_{k,k-1}$ is a transfer operator. Next it is necessary to transfer a residual forcing function such that the solution on grid k is driven by the residuals calculated on grid $k-1$. This can be accomplished by setting

$$P_k = Q_{k,k-1} R_{k-1}(w_{k-1}) - R_k(w_k^{(0)}) \tag{27}$$

whre $Q_{k,k-1}$ is another transfer operator. Then $R_k(w_k)$ is replaced by $R_k(w_k)+P_k$ in the time stepping scheme. Thus, the multistage scheme is reformulated as

$$\begin{aligned} w_k^{(0)} &= w_k^{(0)} - \alpha_1 \Delta t_k [R_k^{(0)} + P_k] \\ \cdots & \\ w_k^{(q+1)} &= w_k^{(0)} - \alpha_{q+1} \Delta t_k [R_k^{(q)} + P_k] \end{aligned} \tag{28}$$

The result $w_m^{(m)}$ then provides the initial data for the grid k+1. Finally, the accumulated correction on grid k has to be transferred back to detailed analysis of multigrid time-stepping schemes is provided elsewhere (50). With properly optimized coefficients multistage time-stepping schemes can be very efficient drivers of the multigrid process. A W cycle of the type illustrated in Fig. 4 proves to be a particularly effective strategy managing the work split between the meshes. In a three-dimensional case the number of cells is reduced by a factor of eight on each coarser grid. On examination of the figure, it can therefore be seen that the work measured in units corresponding to a step on the fine grid is of the order of

$$1 + 2/8 + 4/64 + \ldots < 4/3 \tag{29}$$

Examples of Flow Simulations

Some examples are presented here to illustrate the kind of results that are attainable with these methods. The calculations can be performed on readily accessible equipment, including the mini-supercomputers that are now becoming widely available.

The first example, displayed in Fig. 5, shows the result of a transonic flow calculation for a swept wing. In this case my program FL067 was used to solve the Euler equations on a structured mesh with 192 intervals wrapped around the wing, 32 intervals normal to the wing, and 48 intervals in the spanwise direction, for a total of 294,912 cells. The figure shows the pressure distribution on the upper and lower surfaces measured by the pressure coefficient $C_p = (p - p_\infty)/(\rho q_\infty^2/2)$, with negative C_p, toward the top, following the usual convention in aeronautical science. The triangular shock pattern is clearly visible. This calculation, requiring the solution of coupled nonlinear equations for 1,474,560 unknowns, reached an essentially steady state in 15 multigrid cycles, with the lift converged within 1 part in 1,000. Because the algorithm is explicit it permits concurrent calculations at separate mesh points, so it is fully amenable both to vector processing and to massively parallel computation. The cover shows the vortical flow generated by a delta wing at a high angle of attack. The flow separates off the sharp side edges and rolls up to form vortices which pass over the top of the wing. The associated low pressure is an important mechanism for enhancing the lift of a high-speed aircraft. In the figure the vortices are illustrated by tracking particle paths. (This flow calculation was also performed with FL067, while the mesh generation and the graphic visualization was the work of G. Volpe and M. Siclari, using facilities at the Grumman Corporate Research Center.)

Figure 6 gives an indication of the present state of the art for viscous flow simulation. It shows a comparison between the predicted pressure distribution over the RAE2822 and experimental data obtained in a wind tunnel. These results were obtained by Martinelli, using a new turbulence model based on renormalization group theory (51). Figure 7 shows a comparison between inviscid and viscous flow simulations for the planned Hermes space shuttle in hypersonic flow at Mach 8, and an angle of attack of 30 degrees. While the calculation demonstrates the capability of the LU implicit algorithm (37), the temperatures reached in the flow are high enough that a more complex model ought to be introduced to allow for real gas effects, such as dissociation and chemical reactions.

If computational methods are to be really useful to airplane designers, they must be able to treat extremely complex configurations. A major pacing item of the effort to attain this goal has been the problem of mesh generation. For simple wing body combinations it is possible to generate rectilinear meshes without too much difficulty (52): for more complicated configurations containing, for example, pylon-mounted engines, it becomes increasingly difficult to produce a structured mesh, which is aligned with all solid surfaces. A popular mesh

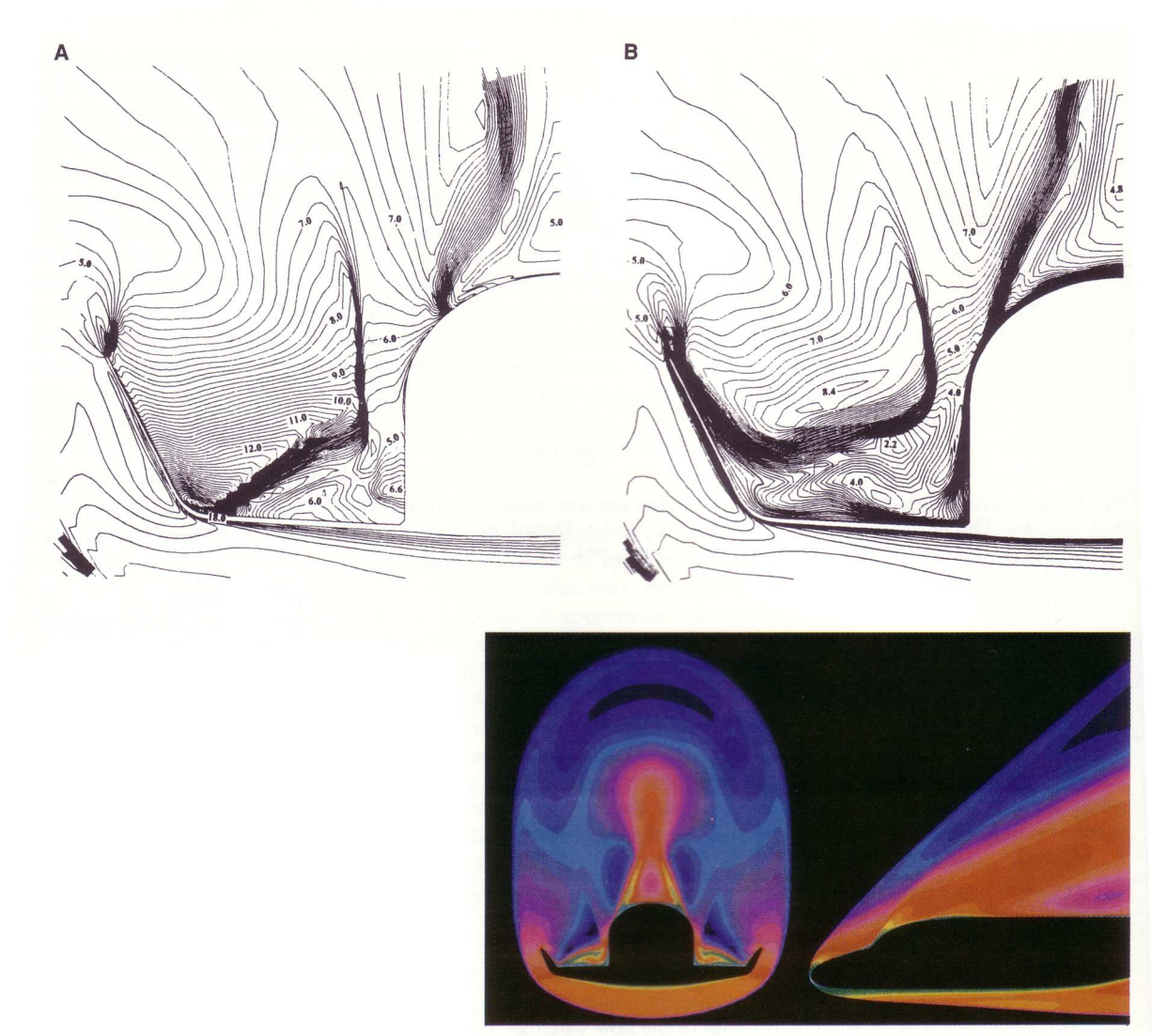

Figure 5: Flow over a design fot the Hermes Space Shuttle at M=8 and 30 degrees angle of attack. Comparison of Mach number distributions for (A) inviscid and (B) viscous flow. (Bottom) The color contours represent the local Mach number, with balck showing the free stream (M=8), yellow-red the range M=3 to 0. (Supplied by H. Rieger, Dornier, GmbH.)

generation procedure, pioneered by Thompson (53), is to generate grid surfaces as solutions of elliptic equations. Hyperbolic marching methods have also proved successful in some applications (54). These methods are typically combined with domain decomposition to produce multiblock meshes in which the mesh inside each block is separately generated. The simulation by Sawada and Takanasha of the flow over a four-engined shorttake off aircraft provides a striking example of what can be achieved by these methods (55).

An alternative procedure is to use tetrahedral cells in an unstructured mesh which can be adapted to conform to the complex surface of an aircraft. Such an approach was successfully implemented for the potential flow equation by Bristeau et al. (13) whose simulation of transonic flow past a complete aircraft was a major advance. Because an arbitrary set of points admits a triangulation, the problem can be simplified by separating the procedure for generating mesh points from the procedure for triangulating them. A cluster of mesh points surrounding the aircraft can be created in any convenient manner. One may take, for example, the union of the points belonging to separately generated meshes around each component. The swarm of mesh points is then connected together to form tetrahedral cells, which provide the basis for a single finiteelement approximation for the entire domain. The triangulation of a set of points to form disjoint tetrahedra is, in general, non-unique: one procedure is to generate the Delaunay triangulation (56, 57). This is dual to the Voronoi diagram that results from a division of the domain into polyhedral neighborhoods, each consisting of the subdomain of points nearer to a given mesh point than any other mesh point.

Combined with a finite-element method based on the concepts outlined in this article, this approach to mesh generation yields an effective method to perform flow calculations for complete aircraft (58, 59). Figure 8 shows a result for the Boeing 747. The color contours denote the surface pressure distribution. The calculation includes internal flow through the engine ducts, but as yet no effort has been made to simulate propulsive effects. Using our Convex C2 mini-supercomputer at Princeton University, we find that calculations with, say, 125,000 to 150,000 nodes and 750,000 to 900,000 tetrahedrons require 15 to 18 hours. We have also been fortunate enough to have been given access to a Cray 2 by Cray Research, which allows us to perform the same calculations in 3 to 4 hours. They also require a lot of memory, typically about 60 million words. Other efforts to develop finite element methods to treat supersonic and hypersonic flows over complex configurations are under way (60, 61).

The Design Problem

In considering the objectives of computational aerodynamics, three levels of desirable performance can be identified: (i) capability to predict the flow past an airplane or its important components in different flight regimes such as take-off or cruise, and off design conditions such as flutter; (ii) interactive calculations to allow rapid improvement of the design; and (iii) integration of the predictive capability into an automatic design method that incorporates computer optimization.

lthough the results presented in this article demonstrate that substantial progress has been made toward the first objective, various problems of viscous separated flows still remain beyond our reach. Also in relatively simple cases, such as an airfoil or wing in inviscid flow, calculations can be performed fast enough that the second objective is attainable. The third objective must eventually prevail. What the designer really needs is a method of determining shapes that will have the desired aerodynamic properties. The ability to predict the flow over a given shape is not good enough for this purpose, as it does not provide any guidance on how to change the shape if it is unsatisfactory. It has been recognized that an experienced designer generally has an idea of the kind of pressure distribution that will lead to favorable characteristics. For example, he can avoid adverse pressure gradients that will induce premature separation of the boundary layer. Thus, in addition to the direct problem of calculating the pressure distribution over a given shape, the inverse problem of finding the shape that will yield a specified pressure distribution can also play an important role. The problem of designing a two-dimensional profile to attain a desired pressure distribution was solved by Lighthill for the case of incompressible flow by means of conformal mapping (62). Subsequently there has been continuing interest in the problem, and a variety of methods have been proposed for the solution of the inverse problem in compressible flow (63-66). One source of difficulty is that the desired pressure distribution is not necessarily attainable, unless it satisfies certain constraints, with the result that the problem needs to be very carefully formulated.

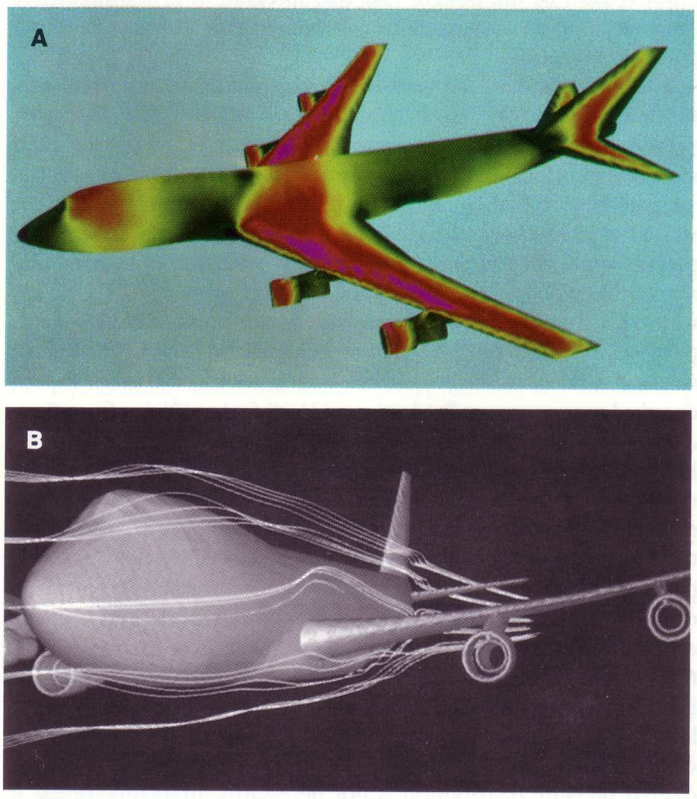

Figure 6: Flow bast a Boeing 747-200 at Mach number 0.84 and 2.73 degrees angle of attack. (Top) The color contours represent the surface pressure, with red indicating low pressure in the supersonic zone. (Bottom) Another view showing streamlines around aircraft. (Calculated by A. Jameson and T. J. Baker.)

The hodograph transformation offers an alternative approach to the design of airfoils to produce shock-free transonic flows. Garabe dian and Korn achieved a striking success by using the method of complex characteristics to solve the equations in the hodograph plane (67). There have been several studies that have explored the possibility of meeting desired design objectives by using constrained optimization (68, 69). The configuration is specified by a set of parameters, and any suitable computer program for flow analysis is used to evaluate the aerodynamic characteristics. In principle this method allows the designer to specify any reasonable design objectives. The method becomes extremely expensive, however, as the number of parameters is increased. In a recent paper I suggested that there are benefits in regarding the design problem as a control problem in which the control is the shape of the boundary (70). A variety of alternative formulations of the design problem can then be treated systematically by using the mathematical theory for control of systems governed by partial differential equations (71).

I have used this approach to accomplish the automatic redesign of airfoils to improve their performance for the case of transonic potential flow. The method proceeds as follows: A two-dimensional profile in the z plane is generated by conformal mapping from a unit circle in the σ plane. Since the transformation is defined by an analytic function, it is fully determined by the value of its modulus $h = |dz/d\sigma|$ on the boundary. Thus we can take f = log h as the control. Suppose now that we define a cost function, such as

$$I = \frac{1}{2}\beta_1 \int_C (p - p_d)^2 d\theta + \beta_2 CD + \frac{1}{2}\beta_3 (CL - CL_d)^2 \tag{30}$$

where the integral is taken over the boundary C, θ is the angle in the circle plane, p is the surface pressure, p_d is the desired surface pressure, CD is the drag coefficient, CL is the lift coefficient, CL_d is the desired lift coefficient, and β_1, β_2 and β_3 are parameters to be chosen by the user. Note that in inviscid flow, minimization of the drag without additional constraints would yield a flat plate at zero angle of attack. Suppose that a perturbation analysis yields an estimate of the variation BI induced by a charge in the mapping function δf of the form

$$\delta I = \int_C g \delta f d\theta \tag{31}$$

where g is independent of δf. Then g can be identified as the gradient or derivative of I with respect to f. If we adjust f by a change

$$\delta f = -\lambda g \tag{32}$$

where λ is any sufficiently small positive variable, then

$$\delta I = -\int_C \lambda g^2 d\theta \tag{33}$$

and the cost must decrease unless the gradient g is already zero, indicating that a stationary point has been attained. At first sight it might appear that one must calculate the change in the solution for each possible change δf. Actually this is not the case. The change $\delta\phi$ in the potential that results from a change δf in the mapping function satisfies an equation of the form

$$L\delta\phi = J \tag{34}$$

where L is the perturbation operator, which is self-adjoint, and J depends on δf. This is a constraint, and we can augment the variation δI by the integral over the domain of this equation multiplied by a Lagrange multiplier Ψ,

$$\int\int_D \psi(L\delta\psi - J) dS \tag{35}$$

Let ψ now be chosen to satisfy the adjoint equation

$$L\psi = 0 \tag{36}$$

with appropriately chosen boundary conditions. Then, an integration by parts, all terms explicitly depending on $\delta\phi$ can be eliminated. In this way it is possible to search for the mapping function f that minimizes I by

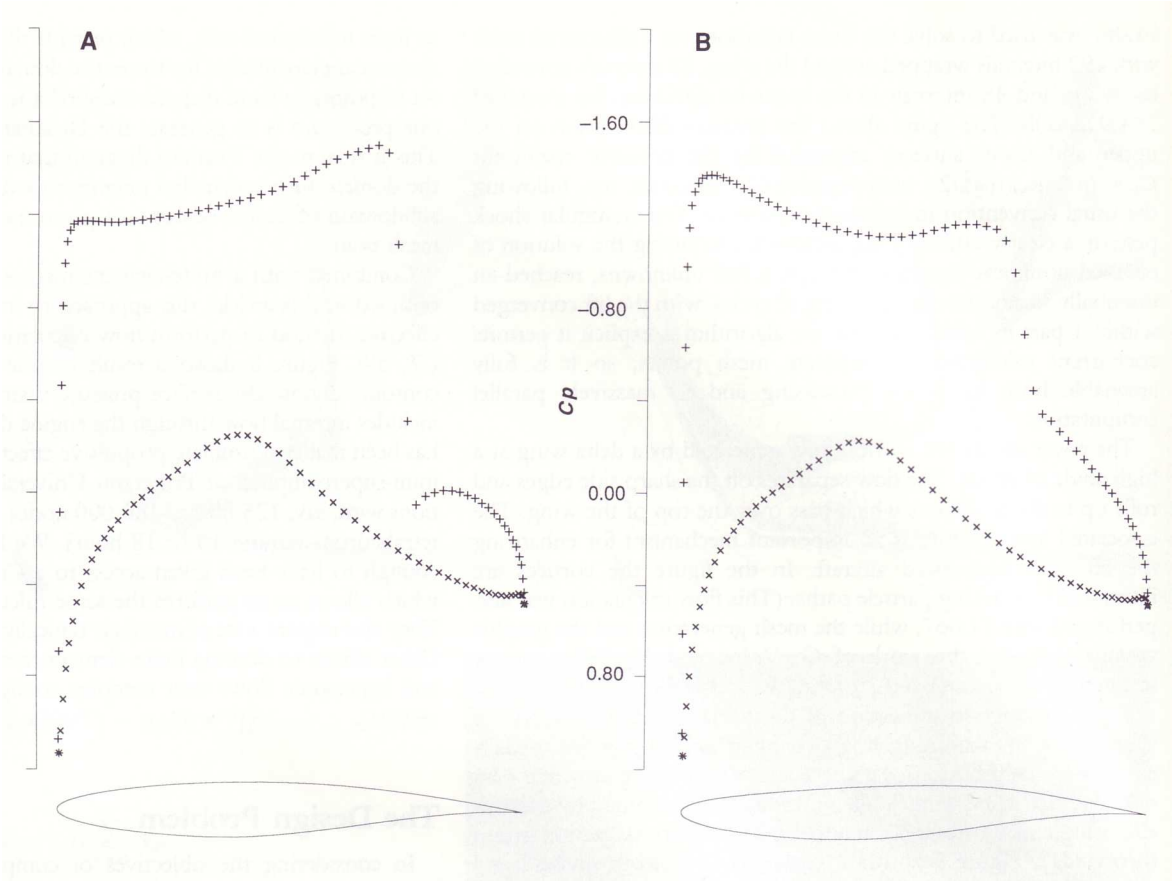

Figure 7: Redesign of the RAE 2822 airfoil by means of control theory to reduce its shock-induced pressure drag. (A) Initial profile. Drag coefficient is 0.0175. (B)Redesigned profile after five cycles. Drag coefficient is 0.0018

an iterative process, in which the flow equation and an adjoint equation of roughly equal complexity must be solved at each iteration.

Figure 9 illustrates a result (previously unpublished) obtained by this method. It shows the automatic redesign of a rather well-known airfoil, the RAE 2822, to reduce its shock-induced pressure drag at a Mach number of 0.730, while the lift is held roughly constant. The figure shows the initial airfoil, and the modified airfoil after five design cycles. The corresponding distribution of the pressure coefficient is also shown. The difference between the upper and lower surface pressures indicates the distribution of lift. It can be seen that during the five cycles the drag coefficient is reduced from an initial value of 0.0175, which would be unacceptably large, to a final value of 0.0018, a reduction by a factor of 10. Each design cycle takes about 9 s on the Convex C2, and the complete calculation requires less than 2 min. It appears entirely feasible to extend this method to the optimization of wings in three-dimensional flow.

Future Possibilities and Challenges

We are now at a point where a variety of efficient algorithms for the solution of the Euler and Navier-Stokes equations have been developed, and the principles underlying their construction are quite well understood.

Progress in viscous flow simulations (72-75) is paced by availability of sufficient computing power, and the need for more reliable turbulence models. Efforts are under way to treat more complex flows. In particular the simulation of internal flows has lagged behind that of external flows. Devices such as compressors and turbines require the treatment of unsteady flows with strong viscous effects. The unsteady flow induced by a helicopter in forward flight is another example of a very complex flow which extends present methods of simulation to the limit of their capabilities. The accurate prediction of hypersonic flow requires the introduction of much more complex models to allow for dissociation and chemical reactions at high temperatures.

There remain many opportunities for improvement. Procedures for automatic refinement of the mesh in regions requiring better resolution are likely to be widely adopted. Such methods have been developed for both rectangular and triangular meshes (60, 61, 7680). The data structures of finite element methods that use unstructured meshes provide a particularly natural framework for adaptive mesh generation adoption as the calculation proceeds. The ideal method would also be capable of providing both a solution and an accompanying estimate of bounds on the error introduced by discretization. The advent of massively parallel computers will force a reappraisal of the trade-offs in the design of algorithms in favor of schemes allowing concurrent calculation. As the simulations increase in complexity the need for sophisticated pre- and post-processing procedures becomes more pressing, and it is becoming increasingly necessary to integrate computer graphics software with numerical simulation methods. Further development of optimization methods should finally allow flow simulations to be exploited to their full potential for improving aerodynamic design.

References

[1] R. T. Jones, Properties of Low Aspect Ratio Pointed Wings at Speeds Below and Above the Speed of Sound, Report TR835 (National Advisory Committee for Aeronautics, Washington, DC, 1946).

[2] W. D. Hayes, Linearized Supersonic Flow, Report AL-222 (North American Aviation, Inc., Los Angeles, CA, 1947).

[3] R. T. Whitcomb, A Study of the Zero L(Drag-Rise Characteristics of Wing-Body Combinations Near the Speed of Sound, Report TR 1273 (National Advisory Commit tee on Aeronautics, Washington, DC, 1956).

[4] H. Schlichting, Boundary Layer Theory (McGraw-Hill, New York, 1968), p. 17.

[5] C. Canuto, M. Y. Hussaini, A. Quarteroni, D. A. Zang, Spectral Methods in Fluid Dynamics (Springer-Verlag, New York, 1987).

[6] H. W. Liepmann and A. Roshko, Elements of Gas Dynamics (Wiley, New York, 1957), p. 193.

[7] J. L. Hess and A. M. O. Smith, Calculation of Non-Ding Potential Flow About Arbitrary Three-Dimensional Bodies, Report ES 40622 (Douglas Aircraft Corp., Long Beach, CA, 1962).

[8] P. E. Rubbert and G. R. Saaris, A General Three-Dimensional Potential Flow Method Applied to V/STOL Aerodynamics, Technical Paper 680304 (Society of Automotive Engineers, Warrendale, PA, 1962).

[9] E. M. Murman and J. D. Cole, AIAA J. 9,114 (1971).

[10] A. Jameson, Commun. Pure. Appl. Math. 27, 283 (1974).

[11] and D. A. Caughey, Numerical Calculation of the Transonic Flow Past a Swept Wing, Report COO-3077-140 (New York University, New York, 1977).

[12] A. Jameson, in Proceedings of the IMA Conference on Numerical Methods in Applied Fluid Dynamics (Academic Press, New York, 1980).

[13] M. O. Bristeau et al., Computer Methods Appl. Mech. Engineering 51, 363 (1985).

[14] A. Jameson, Commun. Pure. Appl. Math. 41, 507 (1988).

[15] S. K. Godunov, Mat. Sbornik 47, 271 (1959) [translated as JPRS 7225 (U.S. Department of Commerce, Washington, DC, 1960)].

[16] J. P. Boris and D. L. Book, J. Comp. Phys. 11, 38 (1973).

[17] B. van Leer, ibid. 14, 361 (1974).

[18] J. L. Steger and R. F. Warming, ibid. 40, 263 (1981).

[19] P. L. Roe, ibid. 43, 357 (1981).

[20] S. Osher and F. Solomon, Math. Comp. 38, 339 (1982).

[21] A. Harten, J. Comp. Phys. 49, 357 (1983).

[22] S. Osher and S. Chakravarthy, SIAM J. Num. Analysis 21, 955 (1984).

[23] P. K. Sweby, ibid., p. 995.

[24] B. K. Anderson, J. L. Thomas, B. van Leer, paper 85-0122 presented at the AIAA 23rd Aerospace Sciences Meeting, Reno, January 1984.

[25] A. Jameson, in Large Scale Computations in Fluid Mechanics (Lectures in Applied Mathematics), B. E. Engquist, S. Osher, R. C. J. Sommerville, Eds. (American Mathematical Society, Providence, 1985), vol. 22, p. 345.

[26] P. D. Lax, Regional Series on Applied Mathematics (Society for Industrial and Applied Mathematics, Philadelphia, 1973), vol. 11.

[27] A. Jameson and P. D. Lax, Conditions for the Construction of Multi-Point Total Variation Diminishing Differences Schemes, MAE Report 1650 (Princeton University, Princeton, NJ, 1984).

[28] S. Osher and S. Chakravarthy, Very High Order Accurate TVD Schemes, ICASE Report 88-44 (Institute for Computer Applications in Science and Engineering, City?, 1984).

[29] C. Hirsch, C. Lacol, H. Decominch, paper 87-1163 presented at the AIAA 8th Computational Fluid Dynamics Conference, Hawaii, June 1987.

[30] K. G. Powell and B. van Leer, paper 89-0095 presented at the AIAA 27th Aerospace Sciences Meeting, Reno, January 1989.

[31] B. Engquist, P. Lotstedt, B. Sjogreen, Math. Comp. 52, 509 (1989).

[32] E. Isaacson and H. B. Keller, Analysis of Numerical Methods (Wiley, New York, 1966), p. 489.

[33] R. W. Beam and R. F. Warming, J. Comp. Phys. 23, 87 (1976).

[34] T. H. Pulliam and J. L. Steger, paper 35-0360 presented at the AIAA 23rd Aerospace Sciences Meeting, Reno, January 1985.

[35] A. Jameson and E. Turkel, Math. Comp. 37, 385 (1981).

[36] S. Yoon and A. Jameson, paper 87-0600 presented at the AIAA 25th Aerospace Sciences Meeting, Reno, January 1987.

[37] H. Rieger and A. Jameson, paper 88-0619 presented at the AIAA 26th Aerospace Sciences Meeting, Reno, January 1988.

[38] R. Chipman and A. Jameson, paper 79-1555 presented at the AIAA 12th Fluid and Plasma Dynamics Conference, Williamsburg, VA, July 1979.

[39] A. Jameson, in Proceedings of the IMA Conference on Numerical Methods in Aeronautical Fluid Dynamics (Academic Press, New York, 1982), p. 29.

[40] A. Jameson, W. Schmidt, E. Turkel, paper 81-1259 presented at the AIAA 14th Fluid and Plasma Dynamics Conference, Palo Alto, CA, June 1981.

[41] A. Rizzi and L. E. Eriksson, J. Fluid Mech. 148, 45 (1984).

[42] A. Jameson, in Numerical Methods in Fluid Dynamics, F. Brezzi, Ed. (Springer Verlag, New York, 1985), p. 156.

[43] R. P. Federenko, USSR Comp. Math. Math. Phys. 4, 227 (1964).

[44] A. Brandt, Math. Comp. 31, 333 (1977).

[45] W. Hackbusch, Computing 20, 291 (1978).

[46] R. H. Ni, AIAAJ. 20,1565 (1982).

[47] A. Jameson, Appl. Math. Comput. 13, 327 (1983).

[48] M. G. Hall, paper presented at IMA Conference on Numerical Methods for Fluid Dynamics, Reading, U.K., April 1985.

[49] P. W. Hernker and S. P. Spekreijse, paper presented at the Oberwolfach Meeting on Multigrid Methods, December 1984.

[50] A. Jameson, in Multigrid Methods II (Lecture Notes in Mathematics Series), W.Hackbusch and U. Trottenberg, Eds. (Springer-Verlag, New York, 1986), p. 166.

[51] L. Martinelli and V. Yakhot, paper 89-1950 presented at the AIAA 9th Computational Fluid Dynamics Conference, Buffalo, June 1989.

[52] T. J. Baker, Appl. Numerical Math. 2, 515 (1986).

[53] J. F. Thompson, F. C. Thames, C. W. Mastin, J. Comp. Phys. 15, 299 (1974).

[54] J. L. Steger and D. S. Chaussee, SIAMJ. Sci. Statistical Computing 1, 431 (1980).

[55] K. Sawada and S. Takanashi, paper 86-0103 presented at the AIAA 24th Aerospace Sciences Meeting, Reno, January 1986.

[56] B. Delaunay, Bull. Acad. Sci. USSR VII: Class Scil. Mat. Nat. 793 (1934).

[57] G. Voronoi, J. Reine Angew. Math. 134, 198 (1908).

[58] A. Jameson, T. J. Baker, N. Weatherill, paper 86-0103 presented at the AIAA 24th Aerosoace Sciences Meetine, Reno, January 1986.

[59] A. Jameson and T. J. Baker, paper 87-0452 presented at the AIAA 25th Aerospace Sciences Meeting, Reno, January 1987.

[60] B. Stoufet, J. Periaux, F. Fezoui, A. Dervieux, paper 87-0560 presented at the AIAA 25th Aerospace Sciences Meeting, Reno, January 1987.

[61] O. Hassan, K. Margan, J. Peraire, paper 89-0363 presented at the AIAA 27th Aerospace Sciences Meeting, Reno, January 1989.

[62] M. J. Lighthill, A New Method of Two Dimensional Aerodynamic Design, ARC Rand Report M 2112 (Aeronautical Research Council, London, 1945).

[63] G. B. McFadden, An Artificial Viscosity Method for the Design of Supercritical Airfoils, Report COO-3077-158 (New York University, New York, 1979).

[64] G. Volpe and R. E. Melnik, Int. J. Numer. Methods Eng. 22, 341 (1986).

[65] P. A. Henne, paper 80-0330 presented at the AIAA 18th Aerospace Sciences Meeting, Pasadena, January 1980.

[66] M. Giles, M. Drela, W. T. Thompkins, paper 85-1530 presented at the AIAA 7th Computational Fluid Dynamics Conference, Cincinnati, 1985.

[67] P. R. Garabedian and D. G. Korn, in Proceedings of the SYNSPADE 1970, B. Hubbard, Ed. (Academic Press, New York, 1971), pp. 253-271.

[68] R. M. Hicks and P. A. Henne, paper 79-0080 presented at the AIAA 17th Aerospace Sciences Meeting, New Orleans, January 1979.

[69] G. B. Constentino and T. L. Holst, Numerical Optimization Design of Advanced Transonic Wing Configurations, Report TM 85950 (National Aeronautics and Space Administration, Washington, DC, 1984).

[70] A. Jameson, ICASE Report 88-64 [J. Sci. Comput., vol. 3 (1988)].

[71] J. L. Lions, Optimal Control of Systems Governed by Partial Differential Equations (Springer-Verlag, New York, 1971).

[72] R. W. MacCormack, paper 85-0032 presented at the AIAA 23rd Aerospace Sciences Meeting, Reno, January 1985.

[73] T. J. Coakely, paper 87-0416 presented at the AIAA 25th Aerospace Sciences Meeting, Reno, January 1987.

[74] T. H. Pulliam, in Numerical Techniques for Viscous Flow Calculations in Turbomachinery Bladings (Von Karman Institute for Fluid Dynamics, Rhode St. Genetic, Belgium, 1986).

[75] M. Berger and A. Jameson, AIAAJ. 23, 561 (1985).

[76] J. F. Dannenhofer and J. R. Baron, paper 86-0495 presented at the AIAA 24th Aerospace Sciences Meeting, Reno, January 1986.

[77] R. Lohner, K. Morgan, J. Peraire, paper 86-0499 presented at the AIAA 24th Aerospace Sciences Meeting, Reno, January 1986.

[78] D. G. Holmes and S. A. Lamson, Proceedings of the International Conference on Numerical Grid Generation in Computational Fluid Dynamics, Landshut, July 1986.

[79] J. T. Oden et al., Proceedings of the ASME Winter Meeting, Computational Mechanics Advances and Trends, Anaheim, CA, December 1986.

[80] D. Mavriplis and A. Jameson, in Multigrid Methods, Theory, Applications and Supercomputing, S. MacCormick, Ed. (Dekker, New York, 1988).